Numerical Calculations of Off-Resonance Heating

J. C. SPROTT
Oak Ridge National Laboratory, Oak Ridge, Tennessee 37830
(Received 31 March 1972)

The off-resonance heating that is observed in hot-electron plasmas is explained in terms of harmonic resonances, appropriately modified to include relativistic and Doppler effects. A theoretical expression for the heating rate is proposed and is found to agree with the results of a computer simulation over a range of parameters. The theoretical heating rate is evaluated numerically for several special cases, including a uniform magnetic field, a mirror field with a 2:1 mirror ratio, and a large-aspect ratio bumpy torus. The enhanced axial loss observed experimentally with heating below the cyclotron frequency is explained by absorption at harmonics of the electron bounce frequency.

I. INTRODUCTION

Electron cyclotron heating has become a widely used technique for producing and heating plasmas in a variety of magnetic field configurations. The observed heating rates are consistent with theoretical predictions, although detailed quantitative comparisons have not been made. More recently, Dandl *et al.*[1] have shown that microwave power at frequencies well above the cold-electron cyclotron frequency can efficiently heat relativistic electron plasmas in simple mirror systems. This off-resonance heating is beneficial for suppressing certain microinstabilities that occur when resonance heating alone is used. Off-resonance heating has also been observed in mirror/quadrupoles at Oak Ridge[2] and in a mirror[3] and toroidal octopole[4] at Wisconsin. Microwave heating below the cold-electron cyclotron frequency is observed to produce enhanced axial losses in the mirror devices.[1,3]

The earliest theoretical calculation of off-resonance heating was done by Grawe[5] who hypothesized that the electrons lose coherence with the applied rf electric field in a time equal to the bounce time between the mirrors. His result agrees with other calculations in the limit of resonance heating, but grossly underestimates the heating for frequencies well above resonance. Kawamura *et al.*[6] calculated the heating at harmonic resonances, and Eldridge[7] included, in addition, the shift of the resonances due to the relativistic mass increase and Doppler effect.

The purpose of this paper is to show that the observed off-resonance heating can be explained in terms of harmonic resonances, appropriately modified to include relativistic and Doppler effects. The predicted heating rate is compared with the results of a computer simulation over a range of parameters. The heating rate is then evaluated numerically for several special cases.

II. THEORY

Electron cyclotron heating rates can be determined either by integrating the equation of motion of a particle along its trajectory[8] or by integrating the local heating rate as determined from the plasma conductivity along a field line.[4] In the cold-plasma limit, the results are the same, and the perpendicular heating rate can be written as

$$d\bar{W}/dt=\pi e\int E_\perp{}^2 n(\mathbf{r})\delta(B-B_0)\,d\mathbf{r}/2\int n(\mathbf{r})\,d\mathbf{r}, \quad (1)$$

where $E_\perp$ is the rms component of the rf electric field at frequency ω perpendicular to the dc magnetic field $\mathbf{B}(\mathbf{r})$, $n(\mathbf{r})$ is electron density, and B_0 is the magnitude of the magnetic field at the cyclotron resonance ($B_0=m\omega/e$). This equation has a simple physical interpretation since the heating rate is proportional to the average density in the resonance region divided by the average density throughout the volume. Note that the heating rate is energy independent and that no heating is expected in the absence of a resonance.

For a high-mode cavity (many wavelengths across), the electric field is approximately isotropic on the resonance surface, and the $E_\perp$ in the integral can be factored out and replaced with its spatial rms value $\overline{E_\perp{}^2}$ ($\sim 2\overline{E^2}/3$). The electric field is assumed to be locally unperturbed by the plasma, and the calculation is therefore limited to low densities such that

$$\omega_p{}^2=ne^2/\epsilon_0 m\ll\begin{cases}\omega c\mid\nabla B\mid_0/B_0\\ \omega^2.\end{cases}$$

For a cavity the over-all electric field must be calculated self-consistently using the input power and the perturbed Q. The result[4] is to show that above a certain density ($\omega_p{}^2\sim\omega^2/Q_0$, Q_0=unperturbed Q), the plasma dominates the cavity Q and total absorption is expected.

Equation (1) was compared with the result of a computer simulation in an earlier publication.[9] The simulation code calculated the guiding center trajectories of a collection of noninteracting, nonrelativistic electrons near the axis of a spatially sinusoidal, dc magnetic field in the presence of a spatially homogeneous, perpendicular rf electric field. The computed heating wave was in good agreement with the theoretical prediction.

A particle of finite energy experiences a resonance at

the Nth harmonic when

$$\omega = N\omega_c/\gamma + k_{||}v_{||}, \tag{2}$$

where ω_c is the cold-electron cyclotron frequency ($=eB/m$), $k_{||}$ and $v_{||}$ are the components of the wave vector and velocity parallel to $\mathbf{B}$, and $\gamma=(1-v^2)^{-1/2}$. The δ function in Eq. (1) must then be replaced by $\delta[NB-\gamma B_0(1-k_{||}v_{||}/\omega)]$. The heating rates for the various harmonics are weighted according to the Bessel function[6,7] $J_{N-1}^2(\gamma k_\perp v_\perp/\omega)$, whose argument is the order of the gyroradius divided by the rf wavelength. The heating rate for a distribution of electrons is obtained by summing the harmonics and integrating over the electron distribution function $f(\mathbf{r}, \mathbf{v})$:

$$\frac{d\bar{W}}{dt} = \pi e\overline{E_\perp^2} \iiint \sum_{N=1}^{\infty} f(\mathbf{r}, \mathbf{v}) J_{N-1}^2\left(\frac{\gamma k_\perp v_\perp}{\omega}\right) \delta\left[NB-\gamma B_0\left(1-\frac{k_{||}v_{||}}{\omega}\right)\right] dk_{||}\, d\mathbf{v}\, d\mathbf{r} \Big/ 2\iiint f(\mathbf{r}, \mathbf{v})\, dk_{||}\, d\mathbf{v}\, d\mathbf{r}. \tag{3}$$

In the above equation the electric field is assumed to be isotropic so that the parallel wave vectors are distributed uniformly over the interval $-k<k_{||}<k$, where

$$k=\omega/c=(k_\perp^2+k_{||}^2)^{1/2}.$$

Equation (3) can then be used to find the average heating rate for an arbitrary plasma provided the distribution function $f(\mathbf{r}, \mathbf{v})$ and field shape $\mathbf{B}(\mathbf{r})$ are known. The general problem of finding the time evolution of $f(\mathbf{r}, \mathbf{v})$ is more difficult since it requires a solution of the Boltzmann equation with a collision term calculated from the heating rate using the Fokker–Planck equation.

III. COMPUTER SIMULATION

A computer code was written to calculate the trajectories and average kinetic energy of a collection of noninteracting electrons in an external dc magnetic field and an external rf electromagnetic field. The fields are given by

$$E_x = E_0 \sin\omega t(\sin ky+\cos kz),$$

$$E_y = E_0 \sin\omega t(\sin kz+\cos kx),$$

$$E_z = E_0 \sin\omega t(\sin kx+\cos ky),$$

$$B_x = \frac{(1-R)x}{4L} B(0)\left(1+\frac{r^2}{8L^2}\right)\sin\frac{z}{L} + \frac{kE_0}{\omega} \times \cos\omega t(\sin ky+\cos kz),$$

$$B_y = \frac{(1-R)y}{4L} B(0)\left(1+\frac{r^2}{8L^2}\right)\sin\frac{z}{L} + \frac{kE_0}{\omega} \times \cos\omega t(\sin kz+\cos kx),$$

$$B_z = \tfrac{1}{2}[B(0)]\left[(1+R)+(1-R)\left(1+\frac{r^2}{4L^2}\right)\cos\frac{z}{L}\right] + \frac{kE_0}{\omega}\cos\omega t(\sin kx+\cos ky).$$

The electric field is the superposition of three, mutually orthogonal, standing waves, which should approximate the field in a high-mode microwave cavity. The magnetic field consists of an infinite series of axisymmetric magnetic mirrors with an axial mirror ratio of R and length $2\pi L$, and of a small, time-varying component chosen to satisfy Maxwell's equations in free space for the rf electric field. The dc magnetic field satisfies $\nabla\cdot\mathbf{B}=0$ exactly and $\nabla\times\mathbf{B}=0$ up to a term of order $(R-1)(r/L)^4/32$. This case was chosen because it should approximately represent the conditions in the proposed large-aspect ratio, high-beta bumpy torus at Oak Ridge.[10] Other field configurations including linear octopoles and mirror/quadrupoles have been simulated, but these cases will not be discussed here. Various initial conditions were used, but for most of the cases described, the particles were initially monoenergetic, isotropic, and distributed with constant density out to the flux surface with a midplane radius of L, which corresponds approximately to the last field line that clears the radial wall in the Elmo[1] device.

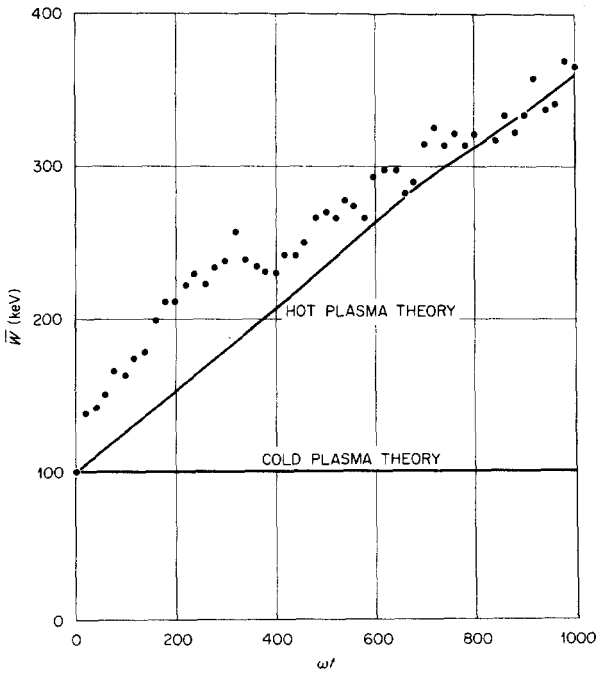

FIG. 1. Typical simulated heating rate for 50 initially isotropic electrons in a 2:1 mirror of length $kL=50$, with $E_0=0.1cB_0$, and $\omega/\omega_c(0)=3$.

The particle trajectories were calculated using the exact, relativistic, three-dimensional equations of motion:

$$(d/dt)(\gamma m\mathbf{v}) = e(\mathbf{E}+\mathbf{v}\times\mathbf{B}).$$

The time interval of the iteration step Δt and the duration of the computer run $t_{\max}$ are typically related to the other characteristic times according to

$$10^4\Delta t \sim 10^3/\omega \sim 10^3/\omega_c \sim 10/\omega_\beta \sim t_{\max},$$

where ω_β is the bounce frequency between the mirrors. The accuracy of the computation was verified by varying Δt and by setting $E_\perp = 0$. The average kinetic energy was calculated by two independent methods:

$$\bar{W}(t) = N_p^{-1}\sum_{i=1}^{N_p} W_i(t),$$

$$= N_p^{-1}\sum_{i=1}^{N_p}\left[e\int_0^t \mathbf{v}_i(t)\cdot\mathbf{E}\,dt + W_i(0)\right],$$

where N_p is the number of particles (typically 50). The two methods generally agree to within a few percent. This computer code represents a considerably more sophisticated version of a code previously used[9] to test the resonance heating predictions of Eq. (1).

In the present version of the code, the theoretical heating rates given by Eqs. (1) and (3) were simultaneously integrated using the distribution function determined from the simulation at each time step in order to derive a theoretical $\bar{W}(t)$. Actually, the distribution function was never determined, but the predicted energy was calculated by the mathematically equivalent method of increasing the predicted average energy by the value of the integrand of Eq. (3) every time a particle satisfied the resonance condition of Eq. (2). For energies below about 100 keV, both the cold-plasma theory of Eq. (1) and the hot-plasma theory of Eq. (3) were found to agree with the results of the simulation to within about a factor of 2 whenever a fundamental resonance was present. For frequencies above resonance, the cold-plasma theory predicts no heating but the hot-plasma theory was found to approximately agree with the simulation as shown, for example, in Fig. 1. About 50 cases were examined covering the range of parameters $0.001 < E_0/cB_0 < 0.1$, $0.5 < \omega/\omega_c(0) < 50$, $0.1 < W < 1000$ keV, $1.01 < R < 100$, and $1 < kL < 1000$. The simulated heating rates were compared with the rates predicted by Eq. (3) and the results are shown in Fig. 2. The average of all the runs gives

$$\log_{10}(\text{theoretical rate/simulated rate}) = -0.044 \pm 0.298,$$

and so the agreement is within about a factor of 2, which may be consistent with the statistics of the simulation, considering the small number of particles that were used.

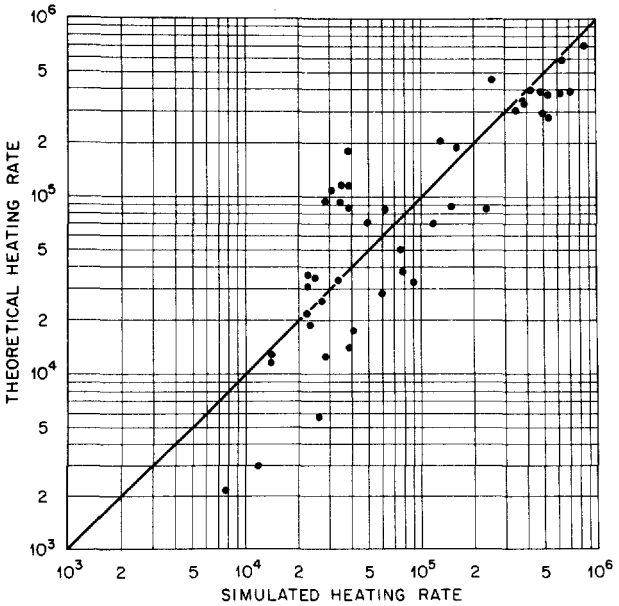

FIG. 2. Comparison of theoretical heating rate calculated from Eq. (3) and simulated heating rate.

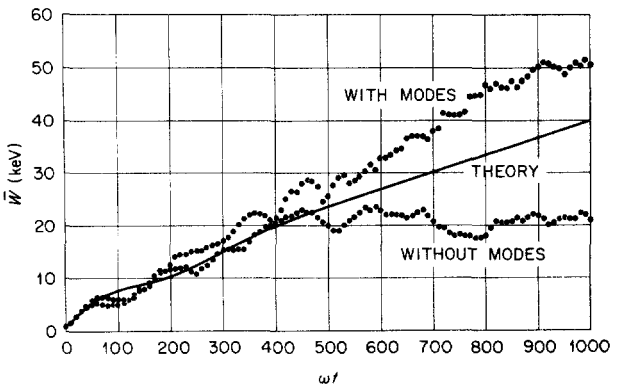

FIG. 3. Average energy vs time, showing saturation for a spatially uniform electric field.

In the earlier, idealized, computer calculation,[9] it was observed that for resonance heating, the particles tended to turn at the resonance surface and a saturation in energy sometimes occurred at high energies. These effects were not observed in the more realistic calculation which includes a spatial variation of **E**, a component of **E** parallel to **B**, and an rf magnetic field consistent with the applied **E** field. These additional effects apparently alter the simple periodic motion that causes a failure of stochasticity. Ultimately, any bounded physical system governed by deterministic equations of motion will be periodic but the time scale for the periodicity increases as the equations become more complicated.[11] An example of this is shown in Fig. 3, where the mode structure of the rf electric field

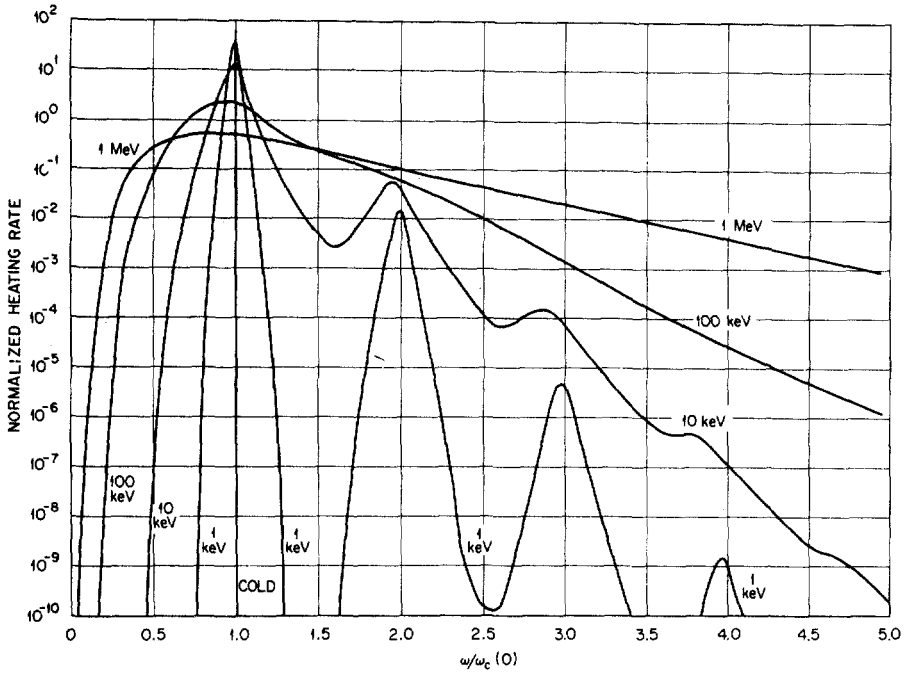

FIG. 4. Heating rate vs rf frequency for a uniform magnetic field.

was removed from the calculation, causing the energy to saturate. Similarly, the turning point distribution is sharply peaked near the resonance for the ideal case, but more uniformly distributed for the realistic case.

The average anisotropy, defined by

$$A = \frac{\sum v_\perp^2/v^2}{2\sum v_{||}^2/v^2}$$

was also calculated as a function of electron energy and microwave frequency. In contrast to the idealized resonance calculation which showed a large anisotropy, the present calculation gives $A \simeq 1$ above 100 keV for all microwave frequencies. Even at low energies ($\lesssim 1$ keV), the maximum anisotropy is $A \simeq 2$ for midplane heating. It was hoped that heating below the fundamental resonance would show $A < 1$, thereby explaining the enhanced axial diffusion observed experimentally.[1,3] Unfortunately, the heating for these cases

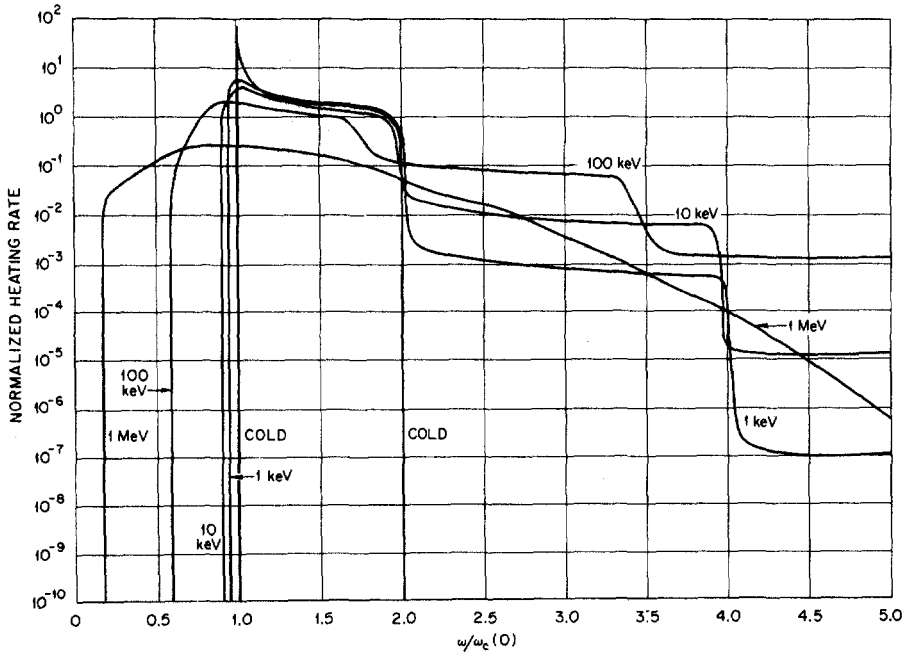

FIG. 5. Heating rate vs rf frequency for a mirror field with 2:1 mirror ratio.

was unobservably small. It may be that the enhanced axial diffusion results when the perpendicular heating vanishes as Eq. (3) predicts below resonance, while the parallel electric fields drive harmonics of the bounce motion, leading to a parallel heating. This hypothesis is examined in more detail in Sec. V.

IV. SPECIAL CASES

Since Eq. (3) correctly predicts the heating rates observed in the computer simulation, it is instructive to examine the predictions for some special cases. For this purpose, the integral in Eq. (3) was evaluated for a variety of $f(\mathbf{r}, \mathbf{v})$ and $\mathbf{B}(\mathbf{r})$. For example, Fig. 4 shows the heating rate as a function of heating frequency for a case in which the magnetic field is spatially uniform and the electrons are isotropic with an energy distribution of

$$f(W) \propto \exp(-W/\bar{W}).$$

The cold-plasma heating rate is a delta function at the fundamental. For $\bar{W}>0$ the harmonics appear and the resonances are broadened as a result of the isotropic distribution of wave vectors, the Doppler effect, and the spectrum of relativistic masses. Above 100 keV, the resonances are washed out, and the heating rate decreases smoothly as the frequency increases. The heating rate is in units of $e\overline{E_\perp^2}/\omega B_0$ (i.e., electron volts per radian). For an electric field of 100 V/cm at a frequency of 10 GHz, one unit represents a heating rate of 2.8×10^8 eV/sec. In these units, we expect total absorption whenever the heating rate exceeds $\omega^2/Q_0\omega_p^2$, and in this limit the electric field adjusts itself so that the actual heating rate is just equal to the input microwave power divided by the number of electrons in the cavity.

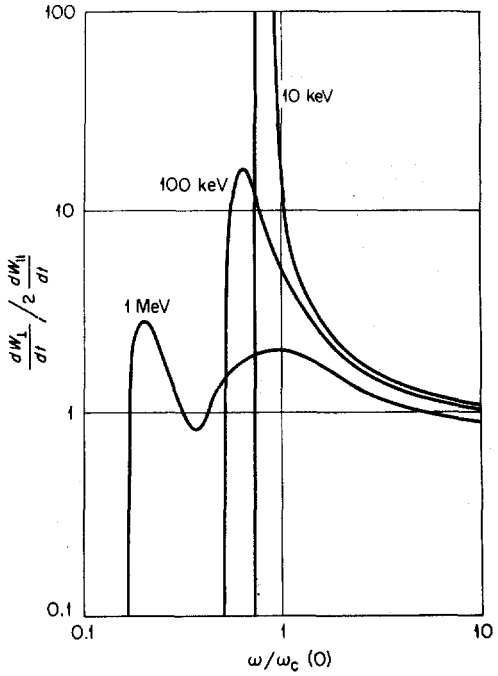

FIG. 7. Ratio of perpendicular to parallel heating for a uniform isotropic plasma in a parabolic mirror.

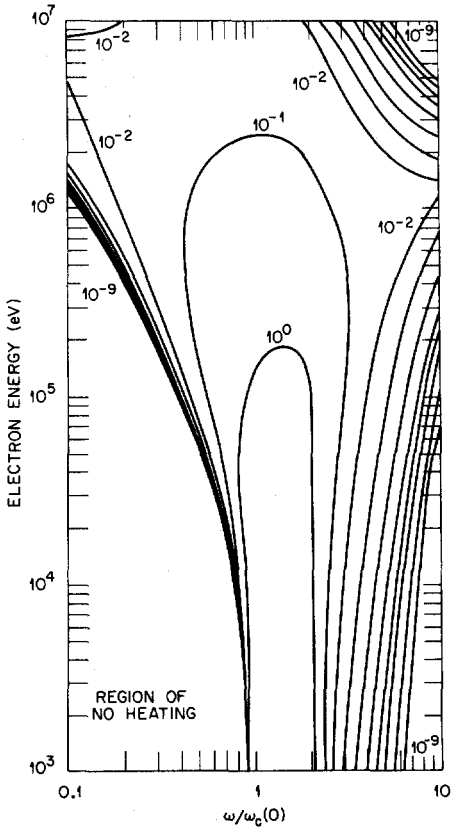

FIG. 6. Contours of constant heating rate for a large-aspect ratio bumpy torus.

Figure 5 shows a case in which the magnetic field is a spatially sinusoidal mirror with a 2:1 mirror ratio. The electrons are distributed with constant density inside a flux tube of infinitesimal cross section centered on the mirror axis. The electrons are monoenergetic and isotropic except for the loss cone which is unpopulated. The spatial and velocity distributions are chosen to be self-consistent in the sense that they represent a steady state on a time scale long compared with the bounce time. Note that cold plasma is heated only over the range of frequencies where a fundamental resonance is present $[1<\omega/\omega(0)<2]$. At higher energies the heating decreases in steps as successively higher harmonics dominate.

Figure 6 shows a similar case but displayed as a plot of contours of constant heating rate as a function of electron energy and heating frequency. The magnetic field is an axisymmetric sinusoidal mirror with a 2:1 axial mirror ratio, and the electrons are isotropic and

monoenergetic and distributed with constant density out to a flux surface well off axis. This case is of interest because it approximates the proposed high-beta bumpy torus at Oak Ridge.

V. PARALLEL HEATING

The discussion thus far has concerned perpendicular heating, since the heating mechanism depends on the cyclotron motion. In a nonuniform magnetic field, parallel heating can also occur. Three such mechanisms will be considered here, and it will be shown that at sufficiently low frequencies, the parallel heating exceeds the perpendicular heating, providing a possible explanation of the enhanced axial losses observed experimentally.

Consider a parabolic mirror field of the form

$$B(z)=B(0)\,(1+z^2/L^2),$$

in which electrons execute sinusoidal bounce oscillations with a frequency of

$$\omega_\beta=L^{-1}[2\mu B(0)/m]^{1/2},$$

where μ is the magnetic moment,

$$\mu=mv_\perp^2/2B.$$

If μ is conserved except within a narrow region of z where perpendicular heating causes μ to change abruptly by an amount $\Delta\mu$ $(=B\Delta W_\perp)$, then the change in parallel energy averaged over a bounce period is

$$\Delta\bar{W}_{||}=\tfrac{1}{2}\Delta[W-W_\perp(0)]=\tfrac{1}{2}[\Delta W_\perp-B(0)\Delta\mu]$$
$$=\tfrac{1}{2}[1-B(0)/B]\Delta W_\perp.$$

A parallel heating then always accompanies a perpendicular heating in a nonuniform field as a result of the $\mu\nabla_{||}B$ force which couples the perpendicular and parallel motion. It is this parallel heating that causes a cold electron initially turning at the resonant surface to continue turning there as its perpendicular energy increases.

A second parallel heating mechanism arises whenever a parallel rf electric field is present, as it must be in a high-mode microwave cavity. This parallel field drives harmonics of the bounce motion just as the perpendicular field drives the cyclotron motion. The resulting parallel heating rate is given by an expression similar to Eq. (3), but with the cyclotron frequency replaced by the bounce frequency. A similar calculation has been used to explain the anomalous loss of electrons from the Van Allen belts,[12] as well as trapped particle effects in tokamaks.[13,14]

The third mechanism is a resonance interaction whereby a particle with finite gyroradius experiences an acceleration from the parallel rf electric field as it crosses a region of cyclotron resonance. Eldridge[7] has calculated that the heating rate for this mechanism is proportional to $J_N^2(\gamma k_\perp v_\perp/\omega)$.

The resulting parallel heating rate from all three mechanisms is given by

$$\frac{dW_{||}}{dt}=\pi e\overline{E_\perp^2}\iiint\sum_{N=1}^{\infty}\left(1-\frac{B(0)}{B}\right)f(\mathbf{r},\mathbf{v})J_{N-1}^2\left(\frac{\gamma k_\perp v_\perp}{\omega}\right)\delta\left[NB-\gamma B_0\left(1-\frac{k_{||}v_{||}}{\omega}\right)\right]dk_{||}\,d\mathbf{v}\,d\mathbf{r}\Big/4\iiint f(\mathbf{r},\mathbf{v})\,dk_{||}\,d\mathbf{v}\,d\mathbf{r}$$
$$+\pi e\overline{E_{||}^2}\iiint\sum_{N=1}^{\infty}f(\mathbf{r},\mathbf{v})J_{N-1}^2\left(\frac{\gamma k_{||}v_{||}}{\omega_\beta}\right)\delta\left(\frac{N\omega_\beta}{\omega}-\gamma\right)dk_{||}\,d\mathbf{v}\,d\mathbf{r}\Big/2B_0\iiint f(\mathbf{r},\mathbf{v})\,dk_{||}\,d\mathbf{v}\,d\mathbf{r}$$
$$+\pi e\overline{E_{||}^2}\iiint\sum_{N=1}^{\infty}f(\mathbf{r},\mathbf{v})J_N^2\left(\frac{\gamma k_\perp v_\perp}{\omega}\right)\delta\left[NB-\gamma B_0\left(1-\frac{k_{||}v_{||}}{\omega}\right)\right]dk_{||}\,d\mathbf{v}\,d\mathbf{r}\Big/2\iiint f(\mathbf{r},\mathbf{v})\,dk_{||}\,d\mathbf{v}\,d\mathbf{r}. \quad (4)$$

Equation (4) was integrated numerically along with Eq. (3) for a parabolic mirror with $kL=1$, and an isotropic monoenergetic distribution with constant density inside a flux surface. The ratio of perpendicular to parallel heating rate for $\overline{E_\perp^2}=2\overline{E_{||}^2}$ is shown in Fig. 7 as a function of heating frequency for several energies. Well above resonance, the anisotropy vanishes. Near resonance the perpendicular heating dominates, especially at low energies, while below resonance the parallel heating dominates. This result resembles the prediction of a collisional, cold-plasma, uniform-field calculation published earlier.[3]

Although the parallel heating below resonance is several orders of magnitude smaller than the resonance heating rates, the perturbed cavity Q is much higher in the absence of cyclotron resonance and the electric field rises in order to maintain total absorption of the microwaves. Whether or not the proposed mechanisms account quantitatively for the observed axial losses can be determined only by more detailed experimental measurements.

VI. CONCLUSIONS

The experimentally observed off-resonance heating can be understood in terms of harmonic resonances, appropriately modified to include relativistic and Doppler effects. The cold-plasma resonance heating theory has been generalized to include these effects,

but the resulting equation is sufficiently complicated so as to require numerical evaluation for special cases. The theoretical heating rate has been compared with the results of a computer simulation, and the agreement is about a factor of 2 over a wide range of parameters. The theoretical heating rate has been evaluated for several special cases. The parallel heating rate was also calculated, and it was shown to exceed the perpendicular heating rate at low frequencies, providing an explanation for the experimentally observed enhanced axial losses. This calculation represents a first step toward the prediction of a self-consistent, time-dependent distribution function for an experimental device using resonant and off-resonant microwave heating. In the laboratory experiments, other mechanisms not included in the simulation, such as collisions or collective effects, may contribute to the heating, but at least for the more relativistic plasmas, the harmonic effects are sufficiently strong to account qualitatively for the observations.

ACKNOWLEDGMENTS

It is a pleasure to acknowledge the many helpful discussions with O. C. Eldridge, G. E. Guest, R. A. Dandl, A. C. England, and G. R. Haste.

This work was supported by the U. S. Atomic Energy Commission under contract with the Union Carbide Corporation.

[1] R. A. Dandl, H. O. Eason, P. H. Edmonds, and A. C. England, Nucl. Fusion **11**, 411 (1971).
[2] W. B. Ard, R. A. Blanken, R. J. Colchin, J. L. Dunlap, G. E. Guest, G. R. Haste, C. L. Hedrick, N. H. Lazar, J. F. Lyon, D. J. Sigmar, and O. B. Morgan, in *Plasma Physics and Controlled Nuclear Fusion Research* (International Atomic Energy Agency, Vienna, 1971), Vol. 2, p. 619.
[3] J. C. Sprott, K. A. Connor, and J. L. Shohet, Plasma Phys. **14**, 269 (1972).
[4] J. C. Sprott, Phys. Fluids **14**, 1795 (1971).
[5] H. Grawe, Plasma Phys. **11**, 151 (1969).
[6] T. Kawamura, H. Momota, C. Namba, and Y. Terashima (to be published).
[7] O. Eldridge, Bull. Am. Phys. Soc. **17**, 773 (1972).
[8] A. F. Kuckes, Plasma Phys. **10**, 367 (1968).
[9] J. C. Sprott and P. H. Edmonds, Phys. **14**, 2703 (1971).
[10] R. A. Dandl, H. O. Eason, P. H. Edmonds, A. C. England, G. E. Guest, C. L. Hedrick, J. T. Hogan, and J. C. Sprott, in *Plasma Physics and Controlled Nuclear Fusion Research* (International Atomic Energy Agency, Vienna, 1971), Vol. 2, p. 607.
[11] H. Poincaré, Acta Math. **13**, 1 (1890).
[12] C. S. Roberts and M. Schulz, J. Geophys. Res. **73**, 7361 (1968).
[13] M. Dobrowolny and O. P. Pogutse, Phys. Rev. Letters **25**, 1608 (1970).
[14] M. Dobrowolny and P. Negrini, Phys. Rev. Letters **28**, 132 (1972).